Journal of Economic Entomology, XX(XX), 2024, 1–8 https://doi.org/10.1093/jee/toae117 Research





Sampling and Biostatistics

Detection of bean damage caused by *Epilachna varivestis* (Coleoptera: Coccinellidae) using drones, sensors, and image analysis

Roghaiyeh Karimzadeh^{1,2}, Kushal Naharki^{1,0}, Yong-Lak Park^{1,*,0}

¹Division of Plant and Soil Sciences, West Virginia University, Morgantown, WV, USA, ²Department of Plant Protection, Faculty of Agriculture, University of Tabriz, Tabriz, Iran *Corresponding author, mail: yopark@mail.wvu.edu

Subject Editor: Dominic Reisig

Received on 3 January 2024; revised on 30 April 2024; accepted on 8 May 2024

The Mexican bean beetle, Epilachna varivestis Mulsant (Coleoptera: Coccinellidae), is a key pest of beans, and early detection of bean damage is crucial for the timely management of E. varivestis. This study was conducted to assess the feasibility of using drones and optical sensors to quantify the damage to field beans caused by E. varivestis. A total of 14 bean plots with various levels of defoliation were surveyed aerially with drones equipped with red-blue-green (RGB), multispectral, and thermal sensors at 2 to 20 m above the canopy of bean plots. Ground-validation sampling included harvesting entire bean plots and photographing individual leaves. Image analyses were used to quantify the amount of defoliation by E. varivestis feeding on both aerial images and ground-validation photos. Linear regression analysis was used to determine the relationship of bean defoliation by E. varivestis measured on aerial images with that found by the ground validation. The results of this study showed a significant positive relationship between bean damages assessed by ground validation and those by using RGB images and a significant negative relationship between the actual amount of bean defoliation and Normalized Difference Vegetation Index values. Thermal signatures associated with bean defoliation were not detected. Spatial analyses using geostatistics revealed the spatial dependency of bean defoliation by E. varivestis. These results suggest the potential use of RGB and multispectral sensors at flight altitudes of 2 to 6 m above the canopy for early detection and site-specific management of E. varivestis, thereby enhancing management efficiency.

Key words: unmanned aerial vehicle, damage assessment, optical sensor, site-specific pest management, remote sensing

Introduction

The Mexican bean beetle, *Epilachna varivestis* Mulsant (Coleoptera: Coccinellidae), is a phytophagous ladybeetle species that invaded the United States in the late 1800s (Nottingham et al. 2016). Beans of the genus *Phaseolus*, including snap beans, lima beans, and pole beans, serve as primary host crops of *E. varivestis*. Larvae and adults feed primarily on the undersides of the leaves, with a high larval density capable of rapidly defoliating an entire bean field; each larva can consume 30 to 70 cm² of bean foliage before pupation (Turner 1932, Bernhardt and Shepard 1978). The signature of defoliation becomes visually detectable when the upper leaf surface dries out, showing a lace-like, skeletonized appearance. Subsequent damage may extend to the reproductive stage, affecting pods and flowers. Snap beans can usually withstand at least 20% defoliation at the vegetative stage (Nottingham et al. 2016), but this amount varies

depending on the growth stage, variety of beans, and environmental conditions. Beans are more sensitive to insect feeding at the flowering and pod fill stages, and yield loss can occur when defoliation exceeds 10% of beans at the reproductive stage (Fan et al. 1993, Nottingham et al. 2016).

Early detection and assessment of crop damage are critical for timely pest management decisions and quick response to pest outbreaks. Management decision for *E. varivestis* is generally made based on mean defoliation level (Bellinger et al. 1981) and larval densities (Higley and Pedigo 1996), with recommended treatment thresholds at 20% and 10% defoliation before flowering and at the pod stage, respectively (Nottingham et al. 2016). Economic thresholds vary, ranging from 1 to 1.5 larvae per bean plant, necessitating adaptability based on bean variety and growing conditions (Michels and Burkhardt 1981, Barrigossi et al. 2003). Predicting bean damage

based on the number of *E. varivestis* egg masses is also suggested as an alternative sampling strategy because sampling egg masses would allow time for preparing and applying control measures before actual damage occurs (Barrigossi et al. 2003).

Current sampling for detecting and rating crop damage by insect pests largely relies on ground-based surveys, which is hard to achieve in large-scale farming or when resources are limited. To overcome the limitation, alternative methods such as remote sensing and image analysis become popularly used as low-cost and rapid pest survey tools in the context of precision agriculture or smart farming (Subramanian et al. 2021, Park et al. 2023). Remote sensing can be used to detect the signs of insects, such as feeding damage (Riley 1989) and nest structures (Mujinya et al. 2014) because insect feeding activity generally causes loss of biomass, changes in vegetation structure, or plant stress responses. Therefore, such signs could be detected from their spectral reflectance and by calculating vegetation indices (Senf et al. 2017, Meng et al. 2018). Specifically, small unmanned aircraft systems (sUAS; a.k.a., drones) can fly at very lowflight altitudes which allows the acquisition of high-resolution aerial images, making them an ideal tool for early detection and measurement of insect pest damage (Hunt Jr and Rondon 2017, Park et al. 2023). In addition, drones are highly maneuverable and can be equipped with automatic flight control to conduct aerial surveys repeatedly without human intervention. Therefore, in recent years the use of drones has been increased in pest management programs including surveillance and monitoring for the detection of plant diseases (Cai et al. 2023, Chin et al. 2023, Qin et al. 2023), insect pest damage (Hunt and Rondon 2017, Subramanian et al. 2021, Park et al. 2023), and weeds (Esposito et al. 2021, Ercolini et al. 2022, Miller et al. 2022). In addition, drones have been used for applying pesticides (Özyurt et al. 2022, Paul et al. 2023, Vitória et al. 2023), delivering pheromone-based mating disruption products (Qin et al. 2023), releasing sterile insects (Garcia et al. 2022, Marina et al. 2022), and biological control agents (Park et al. 2018, Kim et al. 2021, Lake et al. 2021, Martel et al. 2021).

Recent advances in image processing and analysis tools, coupled with high-resolution imagery obtained by drones, provide a unique opportunity for field image processing capability (Bernaola and Holt 2021). For surveillance of crop damage, drones equipped with optical cameras and sensors acquire high-resolution hyperspectral, multispectral, or red-blue-green (RGB) imagery. Stressed plants reflect light differently compared with healthy ones, especially in the visible (380 to 700 nm) and infrared (700 to 2,500 nm) wavelengths (Carter 1993). For example, healthier leaves absorb more red light and reflect more infrared, and thus spectral reflectance ratios calculated from reflected red and infrared lights can be used potentially to evaluate the condition of canopy cover (Board et al. 2007). In addition, it may be possible to identify areas in a field experiencing damage by insects by calculating canopy reflectance ratios (Hunt and Rondon 2017) such as Normalized Difference Vegetation Index (NDVI), Soil Adjusted Vegetation Index (SAVI), simple ratio (SR), green NDVI (GNDVI), Normalized Difference Infrared Index (NDII), red mode (RM), and Enhanced Vegetation Index (EVI). Among the indices, NDVI is the most widely used (Board et al. 2007, Filho et al. 2020, Xulu et al. 2024). Previous studies used such indices derived from multispectral aerial imagery for water stress detection and yield prediction under different sowing periods and irrigation treatments of common bean (Lipovac et al. 2022, Saravia et al. 2023), rapid and accurate estimation of faba bean yield (Cui et al. 2023), characterization of drought stress in soybean (Zhou et al. 2020), and detection of Colorado potato beetle and potato cyst nematode on potato (Hunt Jr and Rondon 2017, Jindo

et al. 2023). Although these studies provided excellent insights into using drones equipped with spectral sensors and image analysis, there still are some challenges because physiological stressors may depend on the growing stages of the crop and can be affected by environmental conditions and agricultural practices. Even, early detection of pest damage may not be feasible unless high-resolution aerial images are obtained with low-altitude remote sensing.

Small drones equipped with obstacle avoidance sensors can be flown at extremely low-flight heights and thus provide opportunities for directly detecting insects from the sky. Park et al. (2021a) conducted a pioneering investigation into the direct detection of insects from aerial surveys using drone imagery. Cocoons of *Monema flavescens* (Lepidoptera: Limacodidae) on the branches of the Japanese zelkova tree could be detectable when the drone was flown at 3 m above the canopy. Tetila et al. (2020) used drone images to detect and classify various soybean pests and successfully identified them when the drone was flown at 2 m above the canopy. In addition, Park et al. (2021b) reported that flying insects could be detected with thermal sensors because the temperature of the thorax increased due to the heavy use of flight muscles when flying.

The goal of this study was to improve current ground-based field sampling methods for *E. varivestis* on beans by using drones for quantifying bean defoliation by *E. varivestis*. Our specific objectives were to (i) evaluate the feasibility of using RGB, multispectral, and thermal sensors carried by drones and image analysis for the assessment of bean damage by *E. varivestis*, (ii) investigate the possibility of direct detection of *E. varivestis* eggs, larvae, pupae, and adults on aerial images acquired with drones, and (iii) determine the possibility of mapping spatial pattern of bean damage by *E. varivestis* and evaluate the potential of site-specific management of *E. varivestis*. Specifically, the investigation delves into the efficacy of low-altitude drone flights in detecting bean damage caused by *E. varivestis*.

Materials and Methods

Study Site, Crop, and Weather Conditions

This study was conducted in two bean fields located at the Organic Research Farm of West Virginia University in Morgantown, WV (39.64422N, 79.93507W). The field was naturally infested with *E. varivestis*. Fourteen plots, each measuring 0.5 m \times 0.5 m and containing 3 to 4 plants, exhibiting various levels of bean damage caused by *E. varivestis* were selected. Aerial surveys and ground samplings were conducted in July and August during the flowering (10%) and pod fill (90%) stages of the beans when different levels of bean damage caused by *E. varivestis* were observed in the field. The prevailing wind speed ranged from 5 to 12 kph, with air temperatures between 26 and 28 °C, and clear skies during both drone flights and field sampling.

Aerial Surveys with Drones and Sensors

Aerial images were obtained using three different drones that carried three different sensors: the DJI Mavic Mini 3 Pro carrying a 48-megapixel RGB camera (SZ DJI Technology Co., Ltd., Shenzhen, China), DJI Mavic 2 Enterprise Advanced carrying a 3.3-megapixel thermal camera measuring 8 to 14 μ m with 640 × 512 resolution at 30 Hz and a 48-megapixel RGB camera, and DJI Phantom 3 Advanced carrying a multispectral sensor (NDVI Single Sesnor, Sentera, St. Paul, MN) measuring red band (wavelength at 625 nm) and near-infrared band (wavelength at 850 nm). Further details on the specification of the drone and sensor can be found at: DJI Mavic Mini 3 (https://www.dji.com/mini-3/specs), DJI Mavic 2 Enterprise

Advanced (https://enterprise.dji.com/mavic-2-enterprise-advanced/specs), and multispectral sensor (https://sentera.com/hardware/sensors/single/). Because different drones generate different amounts of downward wind which can increase the blurriness of aerial images, we tested what flight height of each drone can blow bean foliage. We found that the Mavic Mini Pro 3 could be flown as low as 2 m above the bean canopy to obtain clear still aerial images. Based on these preliminary test results, Mavic Mini Pro 3 was used to obtain aerial images of bean plots at 2, 3, 4, 5, and 6 m above the canopy, and Mavic 2 Enterprise Advanced was flown at 4 to 20 m above the canopy to capture RGB and thermal images every 1 m. Multispectral images were captured at 2 m above the canopy.

RGB sensors captured natural color images, the thermal sensor generated images with heat signatures, and the multispectral sensor calculated NDVI values. NDVI values were calculated by using a raster calculator in ArcGIS Pro (ESRI, Redland, CA) (Fig. 1). These values were then correlated with bean damage caused by *E. varivestis*. The temperature on aerial images was measured using DJI Thermal Analysis Tool 3 (DJI, Shenzhen, China) (Fig. 2) and plotted against actual bean damage to establish their correlation.

Ground Validation with Whole-Plot Sampling

After acquiring aerial images with drones, all bean plants in each plot were covered carefully with a large plastic bag to prevent *E. varivestis* from escaping. The plants were then cut, and bags were transferred to the laboratory for measuring the amount of defoliation and counting *E. varivestis*. Individual leaves were removed from the plants and spread on a light illuminator to take photos with a camera (NEX-5R, Sony Cop., Chonburi, Thailand) mounted



Fig. 1. An example bean plot A) and corresponding NDVI image B) obtained with drones flown at 2 m above the canopy. The higher value of NDVI indicates a healthier bean canopy.

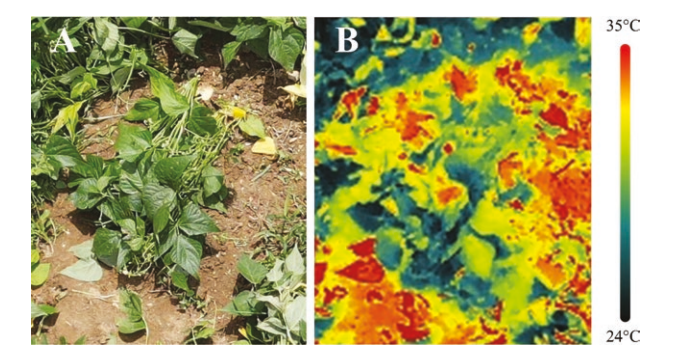


Fig. 2. An example bean plot A) and corresponding thermal image B) obtained with drones flown at 6 m above the canopy.

at 60 cm above the illuminator. These photos were used for image analysis to measure the amount of bean defoliation by *E. varivestis*.

Ability of Aerial Surveys and Image Analysis to Assess Bean Damage

Before image analyses, background elements (i.e., soil and non-bean foliage) were removed from aerial images using Adobe Photoshop CS4 (Adobe Inc., San Diego, CA). ImageJ (National Institutes of Health, Bethesda, MD) was used to measure the total leaf area and defoliated area on each leaf. Different thresholds were selected based on their ability to provide optimal visual differentiation between defoliated and undefoliated pixels on each image. The classification thresholds of RGB images were set for hue of 0-255, saturation of 0-255, and brightness of 0-244 for measuring the total leaf area, and hue of 0-58, saturation of 0-78, and brightness of 0-250 for measuring damaged leaf area (Fig. 3). Although these threshold values were used for most images, a slight modification in values was necessary for some aerial images acquired at different flight heights. We used the same method described above for the analysis of images acquired from the ground-validation sampling except for color thresholds: hue (0-255), saturation (0-255), and brightness (0-224) for measuring leaf area, and hue (0-255), saturation (0-255), and brightness (0-84) (Fig. 4). Wavelengths for red, green, and blue in this study represented 610-760, 500-570, and 450-500 nm, respectively.

Linear regression analysis was conducted to check the ability of aerial surveys and image analysis to assess bean damage. We determine the relationship between actual bean damage measured from ground-validation photos and damage measured from aerial images obtained with different sensors. The regression analysis was conducted with SAS (SAS Institute 2009) to determine the statistical significance of the relationship at $\alpha = 0.05$.

Direct Detection of E. varivestis on Aerial Images

We examined individual aerial images taken from different altitudes to determine if $E.\ varivestis$ eggs, larvae, pupae, or adults could be detected visually on the images acquired with RGB, NDVI, and thermal sensors. All detectable $E.\ varivestis$ on images in each plot were counted and plotted against the actual number of $E.\ varivestis$ counted from the ground-validation photos. Linear regression analysis was used to determine the statistical significance of their relationship at $\alpha=0.05$ by using SAS. In addition, the number of pixels representing individual $E.\ varivestis$ was counted.

Spatial Patterns of Bean Damage by E. varivestis

The possibility of detecting bean damage by using drones and sensors provided an opportunity to generate spatial data on insect pests and conduct spatial analyses. To determine spatial patterns of bean damage by E. varivestis, we used the Mavic 2 Enterprise Advanced to conduct aerial surveys in the two bean fields on the Organic Research Farm of West Virginia University. The drone was flown 6 m above the canopy with autopilot function and aerial images were taken with 80% image overlap between two consecutive aerial images. A total of 46 and 24 aerial images were taken from fields 1 and 2, respectively. The aerial images were downloaded from the drone and stitched using Pix4DMapper software (Pix4D, Prilly, Switzerland) to generate a geo-referenced composite image. The composite image was then processed with Photoshop CS4 to remove background (i.e., soils and non-vegetation) and weeds. Then, image analysis was used to detect damage by E. varivestis throughout the fields by using color thresholds in ImageJ (hue values of 0-255, saturation values of 0–76, and brightness values of 191–231).

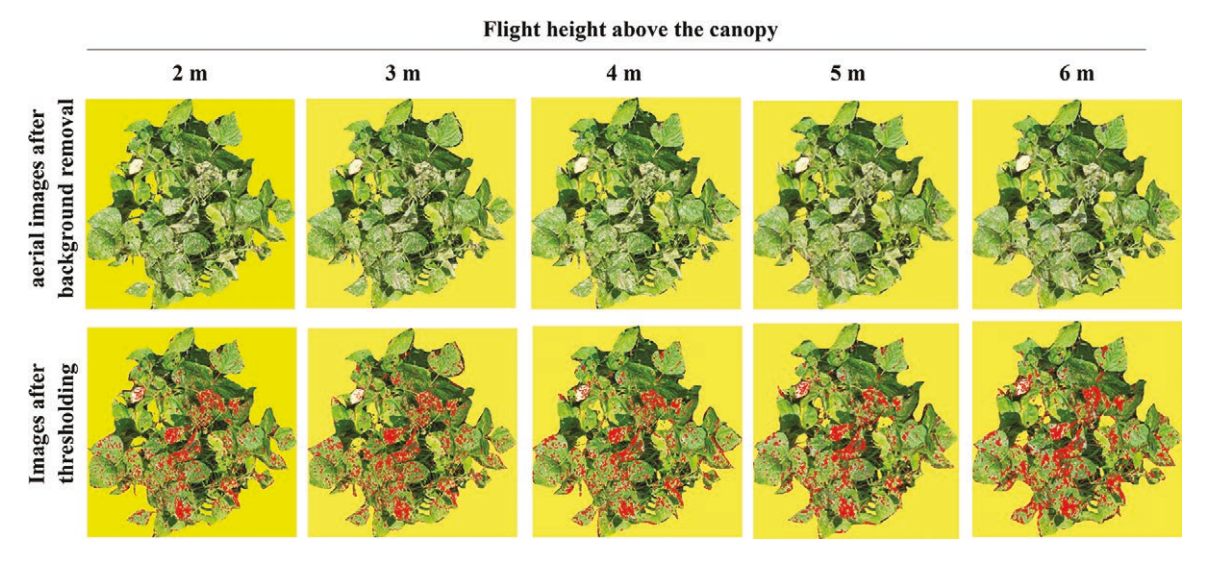


Fig. 3. Processing aerial images acquired with drones at different flight heights to measure the amount of bean defoliation by *Epilachna varivestis*. Background removal (first row) followed by the estimation of bean defoliation (second row) was conducted by thresholding of hue, saturation, and brightness.

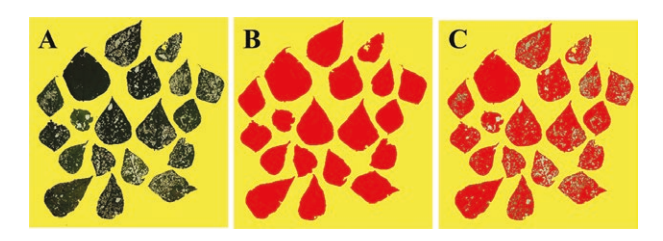


Fig. 4. Processing images of leaves acquired with destructive bean sampling (i.e., on-ground-validation sampling) to measure the total leaf area and the amount of defoliation by *Epilachna varivestis*. Background removal A), total leaf area measurement B), and defoliation estimation C) were conducted by thresholding of hue, saturation, and brightness.

Pixels on the composite images were reclassified into two classes (i.e., damaged and undamaged) using ArcGIS Pro. Using the processed composite image showing pixels for bean damage, we conducted geostatistics analyses to characterize the spatial distribution pattern of bean damage caused by *E. varivestis*. For spatial analysis, the composite image of each field was divided into 500-by-500-pixel grids, and the number of pixels representing *E. varivestis* damage in each grid was counted. A total of 546 and 234 grids were created for fields 1 and 2, respectively. Geostatistical analysis was conducted using the Geostatistical Analysis Extension of ArcGIS Pro, and semivariograms were used to measure the degree of spatial dependency among the number of pixels for defoliation using the formula (Shayestehmehr and Karimzadeh 2019):

Degree of spatial dependency = $[C/(C_0 + C)] \times 100$,

where C is sill and C_0 is the nugget of the semivariogram. Spatial dependency is considered weak, moderate, and strong when the degree of spatial dependency is $\leq 25\%$, 26-75%, and $\geq 76\%$, respectively. Once the spatial dependency or autocorrelation was determined, it was used to produce interpolation maps of bean damage by using kriging.

Results

Ability of Aerial Surveys and Image Analysis to Assess Bean Damage

RGB sensors could detect the feeding signs of *E. varivestis* and bean defoliation up to 6 m above the canopy, although images taken at

lower flight heights provided higher resolution as expected (Fig. 5). The actual amount of damage measured from the ground-validation sampling ranged from 2% to 23%, and the damage measured from areal RGB images ranged from 0.9% to 21% among plots. The mean of damage measured from the ground-validation sampling was $8.1 \pm 1.63\%$, and the mean defoliation levels measured on areal RGB images were $6.9 \pm 1.60\%$, $6.1 \pm 1.38\%$, $5.8 \pm 1.32\%$, $6.2 \pm 1.42\%$, and $6.0 \pm 1.42\%$ for 2, 3, 4, 5, and 6 m above the canopy, respectively.

The results of regression analysis showed that there was a significant positive relationship between actual bean damage and damage assessed from aerial images, and the slope of the linear regression model indicated that 69–85% of actual damage was detected by images obtained with Mavic Mini Pro 3 (Table 1). However, the damage was not detected at flight heights of >6 m with Mavic 2 Enterprise Advanced ($R^2 = 0.074-0.440$, $F_{1,12} = 0.198-0.041$, P = 0.148-0.848). As expected, since *E. varivestis* feeding causes defoliation and vegetation losses, we found a significant negative relationship between NDVI values and the amount of bean defoliation ($R^2 = 0.763$, $F_{1,12} = 38.588$, P < 0.0001). There was no significant difference in temperature between damaged and undamaged bean foliage ($R^2 = 0.111$, $F_{1,4} = 0.4986$, P = 0.5190) according to the thermal image analysis, and the thermal signature of bean defoliation by *E. varivestis* was not detected visually either.

Relationship Between Bean Defoliation and *E. varivestis* Density

A total of 168 larvae (3rd and 4th instars), 164 pupae, and 53 adult *E. varivestis* were found on bean plants harvested from the 14 plots. Regression analysis showed significant relationships of actual bean injury with the total number of *E. varivestis* ($R^2 = 0.872$, $F_{1,12} = 81.99$, P < 0.001) and with the number of larvae ($R^2 = 0.686$, $F_{1,12} = 26.27$, P < 0.001). The slope found in regression analysis indicated that each *E. varivestis* caused 0.45% of bean defoliation. A significant (P < 0.05) and positive relationship was also observed between damage measured from aerial RGB images and the total number of *E. varivestis* at 2–6 m above the canopy (Table 2).

Direct Detection of E. varivestis on Aerial Images

We could detect larvae, pupae, and adults on the RGB images, but NDVI and thermal sensors could not detect the presence of

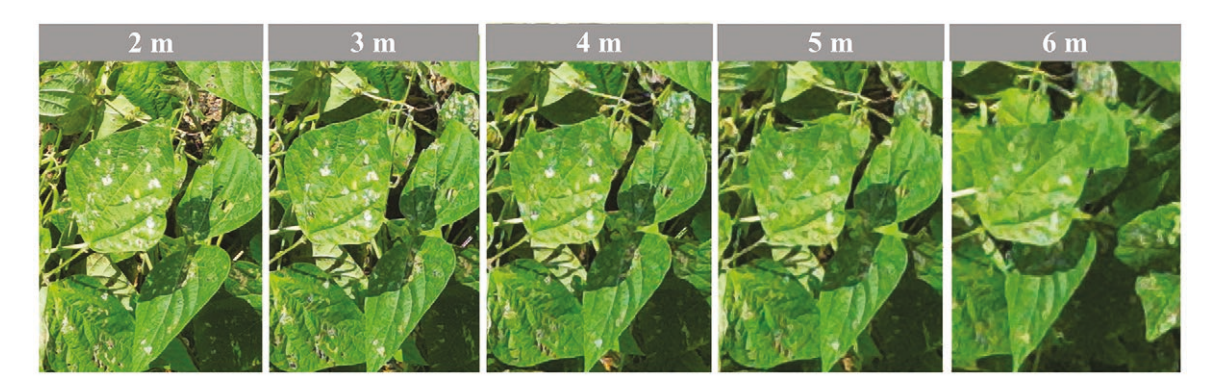


Fig. 5. Resolutions of aerial images taken 2, 3, 4, 5, and 6 m above the canopy of beans with an RGB sensor. All the aerial images represent the same area of the bean canopy.

Table 1. Results of regression analysis showing the relationship between the actual amount of bean defoliation (at %^a) by *E. varivestis* (*x*) and that (at %) assessed by aerial RGB images (y) at five different flight heights

Flight height (m) above the canopy	Regression equation	Degree of freedom	F	P	R^2
2	$y = 0.858 \ x - 0.070$	1, 12	39.27	< 0.0001	0.766
3	$y = 0.757 \ x - 0.020$	1, 12	48.04	< 0.0001	0.800
4	y = 0.631 x + 0.725	1, 12	18.74	0.001	0.609
5	y = 0.753 x + 0.118	1, 12	33.85	< 0.0001	0.738
6	$y = 0.742 \ x + 0.016$	1, 12	32.11	< 0.0001	0.728

^aThe actual damage percentage was calculated for each plot and plotted against the damage percentage assessed by aerial images for that plot.

Table 2. Results of regression analysis showing the relationship between the amount of bean defoliation (at %) assessed by aerial images (RGB) (x) in each plot and the number of E. varivestis (y) in each plot, at five different flight heights

Flight height (m) above the canopy	Regression equation	Degree of freedom	F	P	R^2
2	y = 0.173 x + 2.12	1, 12	11.74	0.005	0.495
3	y = 0.149 x + 2.00	1, 12	11.75	0.005	0.495
4	y = 0.112 x + 2.77	1, 12	5.19	0.040	0.302
5	y = 0.152 x + 2.03	1, 12	11.04	0.006	0.479
6	$y = 0.145 \ x + 2.04$	1, 12	9.51	0.009	0.442

E. varivestis. Each fully-grown *E. varivestis* larva or pupa on the aerial RGB images taken at 3 m above the canopy was represented by 129–153 pixels (Fig. 6). Out of all 385 *E. varivestis* observed in the plots, 20, 10, 2, 0, and 0 were identified in drone images captured at heights of 2, 3, 4, 5, and 6 m above the canopy, respectively. This suggests that the presence of *E. varivestis* could only be detectable in aerial images captured at or below 4 m above the canopy. Although the number of *E. varivestis* detected on aerial images was very low, we still found significant relationships between the number of *E. varivestis* found from the ground validation and that detected on aerial images taken at 2 m ($R^2 = 0.418$, $F_{1,12} = 8.607$, P = 0.013) and 3 m ($R^2 = 0.291$, $F_{1,12} = 4.928$, P = 0.046) above the canopy.

Spatial Patterns of Bean Damage by E. varivestis

The amounts of bean damage measured by image analyses were 4.85% and 2.02% for fields 1 and 2, respectively. The exponential model best fitted the spatial data for field 1 (nugget = 0; sill = 0.82; $R^2 = 0.84$; RSS = 0.0085) and the Gaussian model for field 2 (nugget = 0.39; sill = 0.79; $R^2 = 0.88$; RSS = 0.0095). These models indicate the presence of spatial dependency and moderate to higher degrees of spatial dependence: 100% and 50% in fields 1 and 2, respectively. The interpolated maps of bean defoliation showed that bean defoliation was found across the fields with some hot spots of bean defoliation (Fig. 7).

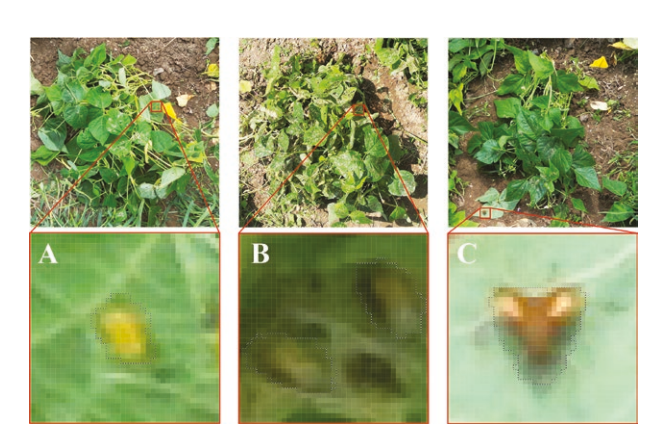


Fig. 6. Direct detection of *Epilachna varivestis* larva A), pupae B), and adult C) on aerial RGB images taken at 2 m above the canopy. Note that the *E. varivestis* adult in (C) was preparing for flight by lifting its forewings.

Discussion

This study aimed to assess the feasibility and potential of utilizing drones equipped with various airborne sensors, including RGB, NDVI, and thermal sensors, to evaluate bean defoliation caused by *E. varivestis*. While such sensors are widely used in precision agriculture for tasks like crop yield prediction and stress detection (Lipovac



Fig. 7. Two bean fields (A and B) for spatial analysis and mapping the distribution of the bean defoliation caused by *Epilachna varivestis*. The spatial distribution of bean defoliation in each field was mapped based on pixels representing defoliation (see "Materials and Methods" section for details), and interpolated maps of bean defoliation were generated by kriging in geostatistics.

et al. 2022), few studies have explored the application of multispectral sensors and NDVI values to detect insect damage in field crops. For instance, Hunt Jr and Rondon (2017) utilized a five-band multispectral sensor to identify Leptinotarsa decemlineata (Coleoptera: Chrysomelidae) damage on potatoes, while Park et al. (2023) employed an RGB sensor for swift detection of bean defoliation during an outbreak of Spodoptera exigua (Lepidoptera: Noctuidae). Our study stands out as the first to evaluate RGB, NDVI, and thermal sensors for the direct detection of various stages of E. varivestis and its feeding signs on beans at low-flight altitudes. The thermal sensor proved ineffective in detecting feeding signs and bean defoliation, although Park et al. (2021b) indicated that flying insects such as bees can be detected with thermal sensors. Both NDVI and RGB images obtained in this study with drones flying at low-flight heights followed by image analysis demonstrated the potential of the rapid and cost-effective detection of bean damage caused by E. varivestis at individual plant and field levels.

Furthermore, our study attempted to use rotary-wing drones equipped with high-resolution cameras at low-flight altitudes (2–4 m above the canopy) in detecting *E. varivestis* larvae, pupae, and adults. Relatively few *E. varivestis* were detected on aerial images because most *E. varivestis* larvae and adults prefer to settle and feed on the underside of the leaf, and eggs are laid on the underside of the leaves. *E. varivestis* was the only coccinellid found in the plots when our destructive sampling was conducted, but the detection of *E. varivestis* with the presence of other coccinellids and similar insects could make the direct detection of *E. varivestis* less accurate.

Our ground sampling results revealed a significant correlation between actual bean damage and the total number of E. varivestis, particularly the 3rd and 4th instars responsible for 87% of bean defoliation (Kabissa and Fronk 1986). These findings can help establish or refine an economic injury level (EIL). Two major components for EIL calculation are I (injury) and D (damage). In the case of defoliators, injury is the amount of defoliation per insect and damage is the economic loss per injury. Because these two components are hard to obtain separately, $I \times D$ is generally obtained with experiments (Pedigo et al. 2021). Two previous studies related insect densities to bean yield without knowing the relationship between defoliation and E. varivestis population density. Barrigossi et al. (2003) used a regression analysis to determine 113 kg/ha per larvae/row-m as the $I \times D$ value, and Capinera et al. (1987) indicated

that dry beans can tolerate a population of 12–20 E. varivestis larvae per plant without significant yield loss. The results of our study indicated that the I value would be $5~\rm cm^2$ per larva from the regression analysis that established a significant positive relationship between damage measured from ground-validation RGB images and the total number of E. varivestis. The I value obtained from this study can help to establish a more realistic EIL for E. varivestis on soybeans.

The outcomes of the spatial analysis substantiated the non-uniform distribution of bean defoliation across the fields. The interpolated maps, depicting bean defoliation by *E. varivestis*, clearly showed the presence of hot and cold spots, denoting areas with high and low defoliation, respectively (Fig. 7). In this scenario, the uniform application of insecticide across the entire field may result in unnecessary treatments in cold spots, thereby diminishing control efficiency. Conversely, implementing site-specific *E. varivestis* control measures in hot spots can significantly enhance efficiency while concurrently reducing control costs. The identification of these distinct defoliation patterns through spatial analysis offers valuable insights for targeted and cost-effective pest management strategies.

While our study emphasizes the potential of RGB and NDVI sensors, image analysis, and spatial analysis for assessing bean damage caused by E. varivestis at individual plant and small-field levels, it also recognizes limitations in surveying large or uneven fields. To address these constraints, we recommend incorporating state-of-the-art drone technology. Firstly, rapid advancements in drone technology enable coverage of large areas for aerial surveys while providing the ability to hover over the target object (i.e., vertical takeoff and landing; VTOL) (Kim et al. 2010). Drones with VTOL capability can serve for both identifying target pests and precisely applying control measures (Cromwell et al. 2021, Rahman et al. 2021). Secondly, low-altitude drone flight facilitates obtaining high-resolution aerial images. Although low-altitude surveys might pose risks, recent developments in anti-collision sensors and global positioning system (GPS) allow drones to be flown at extremely low-flight heights reliably and safely (Parshin et al. 2018, Chandran et al. 2023). Even if the ground is uneven, the drone can maintain a consistent flight altitude above the terrain with terrain-adaptive flight planning using autopilot drone flight with route planning (Silvagni et al. 2017). Lastly, drone swarming, combining advanced anti-collision technology and terrain-following drones, offers potential applications in agriculture to cover larger areas even with

low-altitude drone flights. The coordination of multiple drones flying in synchronized patterns (a.k.a., formation control of drones) can be employed (Mahmood and Kim 2015, He et al. 2018), although this technology has not yet been applied in production agriculture.

In conclusion, this study highlights the potential of highresolution airborne sensors on drones for detecting low-level bean defoliation by *E. varivestis* and directly identifying its various life stages. The findings suggest the potential for generating field maps to guide site-specific management strategies based on defoliation distribution. Moreover, ongoing advancements in drone technology and machine learning can further enhance automated image processing and pest detection accuracy in the future (Chen et al. 2021, Valicharla et al. 2023).

Acknowledgments

We thank S. Deleon and T. Koster (West Virginia University) for their help with field sampling and coordination. This study was supported by the USDA NIFA AFRI Foundational and Applied Science Program (2021-67014-33757) and the West Virginia University Agriculture and Forestry Experiment Station (WVA00785).

Author contributions

Roghaiyeh Karimzadeh (Conceptualization [equal], Data curation [equal], Formal analysis [equal], Investigation [equal], Methodology [equal], Software [equal], Writing – original draft [lead], Writing – review & editing [equal]), Kushal Naharki (Data curation [equal], Formal analysis [equal], Investigation [equal], Software [equal], Visualization [equal], and Yong-Lak Park (Conceptualization [equal], Funding acquisition [lead], Investigation [equal], Methodology [equal], Project administration [lead], Resources [lead], Supervision [lead], Validation [equal], Visualization [equal], Writing – original draft [supporting], Writing – review & editing [lead])

References

- Barrigossi JA, Hein GL, Higley LG. Economic injury levels and sequential sampling plans for Mexican bean beetle (Coleoptera: Coccinellidae) on dry beans. J Econ Entomol. 2003;96(4):1160–1167. https://doi.org/10.1093/jee/96.4.1160
- Bellinger RG, Dively GP, Douglass LW. Spatial distribution and sequential sampling of Mexican bean beetle defoliation on soybeans. Environ Entomol. 1981:10(6):835–841. https://doi.org/10.1093/ee/10.6.835
- Bernaola L, Holt JR. Incorporating sustainable and technological approaches in pest management of invasive arthropod species. Ann Entomol Soc Am. 2021:114(6):673–685. https://doi.org/10.1093/aesa/saab041
- Bernhardt JL, Shepard M. Overwintered Mexican bean beetles: emergence from overwintering sites, fecundity, fertility, and longevity. Ann Entomol Soc Am. 1978:71(5):724–727. https://doi.org/10.1093/aesa/71.5.724
- Board JE, Maka V, Price R, Knight D, Baur ME. Development of vegetation indices for identifying insect infestations in soybean. Agron J. 2007:99(3):650-656. https://doi.org/10.2134/agronj2006.0155
- Cai P, Chen G, Yang H, Li X, Zhu K, Wang T, Liao P, Han M, Gong Y, Wang Q, et al. Detecting individual plants infected with pine wilt disease using drones and satellite imagery: a case study in Xianning, China. Remote Sens. 2023:15(10):2671. https://doi.org/10.3390/rs15102671
- Capinera JL, Horton DR, Epsky ND, Chapman PL. Effects of plant density and late-season defoliation on yield of field beans. Environ Entomol. 1987:16(1):274–280. https://doi.org/10.1093/ee/16.1.274
- Carter GA. Responses of leaf spectral reflectance to plant stress. Am J Bot. 1993:80(3):239–243. https://doi.org/10.1002/j.1537-2197.1993. tb13796.x
- Chandran NK, Sultan MT, Łukaszewicz A, Shahar FS, Holovatyy A, Giernacki W. Review on type of sensors and detection method of anti-collision

- system of unmanned aerial vehicle. Sensors. 2023;23(15):6810. https://doi.org/10.3390/s23156810
- Chen CJ, Huang YY, Li YS, Chen YC, Chang CY, Huang YM. Identification of fruit tree pests with deep learning on embedded drone to achieve accurate pesticide spraying. IEEE Access. 2021;9:21986–21997. https://doi. org/10.1109/access.2021.3056082
- Chin R, Catal C, Kassahun A. Plant disease detection using drones in precision agriculture. Precis Agric. 2023;24(5):1663–1682. https://doi.org/10.1007/s11119-023-10014-y
- Cromwell C, Giampaolo J, Hupy J, Miller Z, Chandrasekaran A. A systematic review of best practices for UAS data collection in forestry-related applications. Forests. 2021;12(7):957. https://doi.org/10.3390/f12070957
- Cui Y, Ji Y, Liu R, Li W, Liu Y, Liu Z, Zong X, Yang T. Faba bean (Vicia faba L.) yield estimation based on dual-sensor data. Drones. 2023:7(6):378. https://doi.org/10.3390/drones7060378
- Ercolini L, Grossi N, Silvestri N. A simple method to estimate weed control threshold by using RGB images from drones. Appl Sci. 2022:12(23):11935. https://doi.org/10.3390/app122311935
- Esposito M, Crimaldi M, Cirillo V, Sarghini F, Maggio A. Drone and sensor technology for sustainable weed management: a review. Chem Biol Technol Agric. 2021;8(1):1–11. https://doi.org/10.1186/s40538-021-00217-8
- Fan Y, Groden E, Liebman M, Alford RA. Response of dry bean yield to injury by Mexican bean beetle (Coleoptera: Coccinellidae) in low-input and conventional cropping systems. J Econ Entomol. 1993:86(5):1574–1578. https://doi.org/10.1093/jee/86.5.1574
- Filho FH, Heldens WB, Kong Z, de Lange ES. Drones: innovative technology for use in precision pest management. J Econ Entomol. 2020:113(1):1–25. https://doi.org/10.1093/jee/toz268
- Garcia M, Maza I, Ollero A, Gutierrez D, Aguirre I, Viguria A. Release of sterile mosquitoes with drones in urban and rural environments under the European drone regulation. Appl Sci. 2022:12(3):1250. https://doi. org/10.3390/app12031250
- He L, Bai P, Liang X, Zhang J, Wang W. Feedback formation control of UAV swarm with multiple implicit leaders. Aerosp Sci Technol. 2018:72:327– 334. https://doi.org/10.1016/j.ast.2017.11.020
- Higley LG, Pedigo LP, editors. Economic thresholds for integrated pest management. Lincoln (Nebraska): University of Nebraska Press; 1996.
- Hunt Jr ER, Rondon SI. Detection of potato beetle damage using remote sensing from small unmanned aircraft systems. J Appl Remote Sens. 2017;11(2):026013. https://doi.org/10.1117/1.JRS.11.026013
- Jindo K, Teklu MG, van Boheeman K, Njehia NS, Narabu T, Kempenaar C, Molendijk LP, Schepel E, Been TH. Unmanned aerial vehicle (UAV) for detection and prediction of damage caused by potato cyst nematode G. pallida on selected potato cultivars. Remote Sens. 2023;15(5):1429. https://doi.org/10.3390/rs15051429
- Kabissa J, Fronk WD. Bean foliage consumption by Mexican bean beetle (Coleoptera: Coccinellidae) and its effect on yield. J Kans Entomol Soc. 1986:59(2):275–279. http://www.jstor.org/stable/25084768
- Kim J, Huebner CD, Reardon R, Park YL. Spatially targeted biological control of Mile-a-Minute weed using *Rhinoncomimus latipes* (Coleoptera: Curculionidae) and an unmanned aircraft system. J Econ Entomol. 2021:114(5):1889–1895. https://doi.org/10.1093/jee/toab020
- Kim J, Kang MS, Park S. Accurate modeling and robust hovering control for a quad-rotor VTOL aircraft. J Intell Robot Syst. 2010:57(1-4):9–26. https:// doi.org/10.1007/s10846-009-9369-z
- Lake EC, David AS, Spencer TM, Wilhelm Jr VL, Barnett TW, Abdel-Kader AA, Carmona Cortes A, Acuna A, Mattison ED, Minteer CR. First drone releases of the biological control agent *Neomusotima conspurcatalis* on Old World climbing fern. Biocontrol Sci Technol. 2021:31(1):97–106. https://doi.org/10.1080/09583157.2020.1828280
- Lipovac A, Bezdan A, Moravčević D, Djurović N, Ćosić M, Benka P, Stričević R. Correlation between ground measurements and UAV sensed vegetation indices for yield prediction of common bean grown under different irrigation treatments and sowing periods. Water. 2022:14(22):3786. https://doi.org/10.3390/w14223786
- Mahmood A, Kim Y. Leader-following formation control of quadcopters with heading synchronization. Aerosp Sci Technol. 2015:47:68–74. https://doi. org/10.1016/j.ast.2015.09.009

- Marina CF, Liedo P, Bond JG, Osorio AR, Valle J, Angulo-Kladt R, Gómez-Simuta Y, Fernández-Salas I, Dor A, Williams T. Comparison of ground release and drone-mediated aerial release of *Aedes aegypti* sterile males in southern Mexico: efficacy and challenges. Insects. 2022:13(4):347. https://doi.org/10.3390/insects13040347
- Martel V, Johns RC, Jochems-Tanguay L, Jean F, Maltais A, Trudeau S, St-Onge M, Cormier D, Smith SM, Boisclair J. The use of UAS to release the egg parasitoid *Trichogramma* spp.(Hymenoptera: Trichogrammatidae) against an agricultural and a forest pest in Canada. J Econ Entomol. 2021:114(5):1867–1881. https://doi.org/10.1093/jee/toaa325
- Meng R, Dennison PE, Zhao F, Shendryk I, Rickert A, Hanavan RP, Cook BD, Serbin SP. Mapping canopy defoliation by herbivorous insects at the individual tree level using bi-temporal airborne imaging spectroscopy and LiDAR measurements. Remote Sens Environ. 2018:215:170–183. https://doi.org/10.1016/j.rse.2018.06.008
- Michels GJ Jr, Burkhardt CC. Economic threshold levels of the Mexican bean beetle on pinto beans in Wyoming. J Econ Entomol. 1981:74(1):5–6. https://doi.org/10.1093/jee/74.1.5
- Miller JO, Shober AL, VanGessel MJ. Post-harvest drone flights to measure weed growth and yield associations. Agric Environ Lett. 2022;7(1):e20081. https://doi.org/10.1002/ael2.20081
- Mujinya BB, Adam M, Mees F, Bogaert J, Vranken I, Erens H, Baert G, Ngongo M, Van Ranst E. Spatial patterns and morphology of termite (*Macrotermes falciger*) mounds in the Upper Katanga, DR Congo. Catena. 2014:114:97–106. https://doi.org/10.1016/j.catena.2013.10.015
- Nottingham LB, Dively GP, Schultz PB, Herbert DA, Kuhar TP. Natural history, ecology, and management of the Mexican bean beetle (Coleoptera: Coccinellidae) in the United States. J Integr Pest Manag. 2016:7(1):2–12. https://doi.org/10.1093/jipm/pmv023
- Özyurt HB, Duran H, Çelen IH. Determination of the application parameters of spraying drones for crop production in hazelnut orchards. J Tekirdag Agric Fac. 2022:19(4):819–828. https://doi.org/10.33462/jotaf.1105420
- Park YL, Cho JR, Choi KH, Kim HR, Kim JW, Kim SJ, Lee DH, Park CG, Cho YS. Advances, limitations, and future applications of aerospace and geospatial technologies for apple IPM. Kor J Appl Entomol. 2021a:60(1):135–143. https://doi.org/10.5656/KSAE.2021.02.0.009
- Park YL, Cho JR, Lee GS, Seo BY. Detection of Monema flavescens (Lepidoptera: Limacodidae) cocoons using small unmanned aircraft system. J Econ Entomol. 2021b:114(5):1927–1933. https://doi.org/10.1093/jee/toab060
- Park YL, Gururajan S, Thistle H, Chandran R, Reardon R. Aerial release of Rhinoncomimus latipes (Coleoptera: Curculionidae) to control Persicaria perfoliata (Polygonaceae) using an unmanned aerial system. Pest Manag Sci. 2018:74(1):141–148. https://doi.org/10.1002/ps.4670
- Park YL, Naharki K, Karimzadeh R, Seo BY, Lee GS. Rapid assessment of insect pest outbreak using drones: a case study with *Spodoptera exigua* (Hübner) (Lepidoptera: Noctuidae) in soybean fields. Insects. 2023:14(6):555. https://doi.org/10.3390/insects14060555
- Parshin A, Grebenkin N, Morozov V, Shikalenko F. Research Note: first results of a low-altitude unmanned aircraft system gamma survey by comparison with the terrestrial and aerial gamma survey data. Geophys Prospect. 2018:66(7):1433–1438. https://doi.org/10.1111/1365-2478.12650
- Paul RA, Arthanari PM, Pazhanivelan S, Kavitha R, Djanaguiraman M. Drone-based herbicide application for energy saving, higher weed control

- and economics in direct-seeded rice (*Oryza sativa*). Indian J Agric Sci. 2023:93(7):704–709. https://doi.org/10.56093/ijas.v93i7.137859
- Pedigo LP, Rice ME, Krell RK. Entomology and pest management. 7th ed. Long Grove (IL): Waveland Press; 2021. p. 584.
- Qin B, Sun F, Shen W, Dong B, Ma S, Huo X, Lan P. Deep learning-based pine nematode trees' identification using multispectral and visible UAV imagery. Drones. 2023;7(3):183. https://doi.org/10.3390/drones7030183
- Rahman MF, Fan S, Zhang Y, Chen L. A comparative study on application of unmanned aerial vehicle systems in agriculture. Agriculture. 2021:11(1):22. https://doi.org/10.3390/agriculture11010022
- Riley JR. Remote sensing in entomology. Annu Rev Entomol. 1989;34(1):247–271. https://doi.org/10.1146/annurev.en.34.010189.001335
- Saravia D, Valqui-Valqui L, Salazar W, Quille-Mamani J, Barboza E, Porras-Jorge R, Injante P, Arbizu CI. Yield prediction of four bean (*Phaseolus vulgaris*) cultivars using vegetation indices based on multispectral images from UAV in an arid zone of Peru. Drones. 2023:7(5):325. https://doi.org/10.3390/drones7050325
- SAS Institute. SAS Proprietary Software Version 9.3. Cary (NC): SAS Institute; 2009.
- Senf C, Seidl R, Hostert P. Remote sensing of forest insect disturbances: current state and future directions. Int J Appl Earth Obs Geoinf. 2017:60:49–60. https://doi.org/10.1016/j.jag.2017.04.004
- Shayestehmehr H, Karimzadeh R. Geostatistical analysis of spatial distribution of *Therioaphis maculata* (Hemiptera: Aphididae) and coccinellid lady beetles (Coleoptera: Coccinellidae). J Crop Prot. 2019:8(1):103–115.
- Silvagni M, Tonoli A, Zenerino E, Chiaberge M. Multipurpose UAV for search and rescue operations in mountain avalanche events. Geomat Nat Hazards Risk. 2017;8(1):18–33. https://doi.org/10.1080/19475705.2016.1238852
- Subramanian KS, Pazhanivelan S, Srinivasan G, Santhi R, Sathiah N. Drones in insect pest management. Front Agron. 2021:3:640885. https://doi. org/10.3389/fagro.2021.640885
- Tetila EC, Machado BB, Astolfi G, de Souza Belete NA, Amorim WP, Roel AR, Pistori H. Detection and classification of soybean pests using deep learning with UAV images. Comput Electron Agric. 2020:179:105836.
- Turner N. The Mexican bean beetle in Connecticut. J Econ Entomol. 1932:25(3):617–620. https://doi.org/10.1093/jee/25.3.617
- Valicharla SK, Li X, Greenleaf J, Turcotte R, Hayes C, Park YL. Precision detection and assessment of ash death and decline caused by the emerald ash borer using drones and deep learning. Plants (Basel, Switzerland). 2023:12(4):798. https://doi.org/10.3390/plants12040798
- Vitória EL, Krohling CA, Borges FR, Ribeiro LF, Ribeiro ME, Chen P, Lan Y, Wang S, Moraes HM, Furtado Júnior MR. Efficiency of fungicide application and using an unmanned aerial vehicle and pneumatic sprayer for control of Hemileia vastatrix and Cercospora coffeicola in mountain coffee crops. Agronomy. 2023;13(2):340. https://doi.org/10.3390/agronomy13020340
- Xulu S, Mbatha N, Peerbhay K, Gebreslasie M, Agjee N. Comparison of different spectral indices to differentiate the impact of insect attack on planted forest stands. Remote Sens Appl Soc Environ. 2024;33:101087. https://doi.org/10.1016/j.rsase.2023.101087
- Zhou J, Zhou J, Ye H, Ali ML, Nguyen HT, Chen P. Classification of soybean leaf wilting due to drought stress using UAV-based imagery. Comput Electron Agric. 2020:175:105576. https://doi.org/10.1016/j.compag.2020.105576